
Article:
Richter, AR, Feitosa, JPA, Paula, HCB et al. (2 more authors) (2018) Pickering emulsion stabilized by cashew gum- poly-l-lactide copolymer nanoparticles: Synthesis, characterization and amphotericin B encapsulation. Colloids and Surfaces B: Biointerfaces, 164. pp. 201-209. ISSN 0927-7765

https://doi.org/10.1016/j.colsurfb.2018.01.023

Pickering emulsion stabilized by cashew gum- poly-L-lactide copolymer nanoparticles: synthesis, characterization and amphotericin B encapsulation

Richter A. R.[a], Feitosa J.P.A.[a], Paula H.C.B.[b], Goycoolea F. M.*[c,d], de Paula R. C. M.*[a]

[a] Federal University of Ceará - Department of Organic and Inorganic Chemistry - CP 12.200, CEP 60455-760, Fortaleza, Ceará, Brazil

[b] Federal University of Ceará, Department of Analytical and Physical Chemistry CP 12.200, CEP 60455-760, Fortaleza, Ceará, Brazil

[c] University of Münster, Institute of Plant Biology and Biotechnology, Schlossgarten 3, D-48149 Münster, Germany.

[d] School of Food Science and Nutrition. University of Leeds. LS2 9JT. Leeds, U.K.

*Corresponding authors: F.M.Goycoolea@leeds.ac.uk; rpaula@dqoi.ufc.br

ABSTRACT

In this work, we provide proof-of-concept of formation, physical characteristics and potential use as a drug delivery formulation of Pickering (PE) emulsions obtained by a novel method that combines nanoprecipitation with subsequent spontaneous emulsification process. To this end, pre-formed ultra-small (d.~10 nm) nanoprecipitated nanoparticles of hydrophobic derivatives of cashew tree gum grafted with polylactide (CGPLAP), were conceived to stabilize Pickering emulsions obtained by spontaneous emulsification. These were also loaded with Amphotericin B (AmB), a drug of low oral bioavailability used in the therapy of neglected diseases such as leishmaniasis. The graft reaction was performed in two CG/PLA molar ratio conditions (1:1 and 1:10). Emulsions were prepared by adding the organic phase (Miglyol 812®) in the aqueous phase (nanoprecipitated CGPLAP), resulting the immediate emulsion formation. The isolation by centrifugation does not destabilize or separate the nanoparticles from oil droplets of the PE emulsion. . Emulsions with CGPLAP 1:1 presented unimodal distributions at different CGPLA concentration, lower values in size and PDI and the best stability over time. The AmB was incorporated in the emulsions with a process efficiency of 20 to 47 %, as determined by UV-VIS. AmB in CGPLAP emulsions is in less aggregated state than observed in commercial AmB formulation.

Keywords: Pickering emulsion; cashew gum; poly-L-lactide; copolymer; nanoparticles; amphotericin B.

INTRODUCTION

The first studies documenting the ability of solid particles to stabilize oil droplets in water were reported by Ramsden and Pickering and date back from more than a century ago [1]. Pickering emulsions, either o/w, w/o or multiple, are singled out from classical ones, as they are stabilized by solid particles and by the absence of surfactants [2]. By avoiding the need of use of synthetic surfactants, Pickering emulsions offer several advantages over their classical counterparts, such as better stability, low toxicity and less pollution to the environment. Over recent years, Pickering emulsions stabilized using different type of particles have been reported. In a study, halloysite nanotubes (HNT)($(Al_2Si_2O_5(OH)_4 \cdot nH_2O)$) molecularly imprinted, that have been developed to extract herbicides from water [3] . The same research group, has recently published other studies based on Pickering emulsion by interfacial molecular imprinting and Pickering emulsion polymerization to recognize bovine hemoglobin using different strategies, namely HNT and magnetic nanoparticles [4], hydroxyapatite hybridized polydopamine polymers [5]; [6] . Another study found evidence of the feasibility to obtain Pickering emulsions responsive to pH changes. These particles are based on polysiloxane microsphere bearing phenolphthalein groups, turned from pink to deep red with the augment of pH from 9 to 12. The emulsions also exhibited doubly pH-responsive property: two emulsification/demulsification processes occurred at pH 9 and pH 12, respectively [7].

Despite the great interest focused on Pickering emulsions stabilized by inorganic and synthetic polymeric particles, only recently researchers have started to account for the use of natural edible polysaccharides, proteins and other natural food constituents for this purpose. Therefore, particulate systems comprising alginate [8], modified starch [9, 10], chitin nanocrystals [11], chitosan [12], cellulose nanocrystals [13-15]; soy protein nanoparticles [16] or whey protein microgels [17] have been reported.

Cashew gum (CG) is an heteropolysaccharide comprised by β-D-galactose (72-73%), α-D-glucose (11-14%), L-arabinose (4,6%), L-ramnose (3-4%), D-glucuronic acid (4-7%) and a small fraction (5-8 %) of protein [18]. The solubility and biodegradability

in physiological conditions of CG, anticipates its amenability and potential use to develop matrices to associate and release low molar mass drugs, biologics and cells [18]. In this paper, we report for the first time, the use of self-assembled nanoparticles of CG grafted with polylactic acid (PLA) obtained by nanoprecipitation, and subsequently its use to obtain stable Pickering emulsions by spontaneous emulsification. Synthesis of CG - poly-L-lactide derivatives were previous described by Reicher [19]. These type of hybrid materials offer improved functional properties in the development of drug delivery formulations [20] including their enhanced biodegradability [21]. We have selected amphotericin B (AmB) (Scheme 1) as the drug to load into the Pickering emulsions. AmB is a potent fungistatic and fungicide drug produced by the actinomycetes Streptomycetes nodosus [22] that was approved for clinical use by FDA in 1959 [23]. AmB is also prescribed in the treatment of visceral leishmaniasis. It is a lipophilic drug that binds to lipids and intercalates into lipid bilayers that then associate to form transmembrane pores [24]. Its selectivity for fungi is associated with its greater affinity for ergosterol than to cholesterol. However, non-selective toxicity towards human erythrocytes is mediated by its state of aggregation [25]. AmB was introduced in the market as a micellar suspension with sodium deoxychlolate (Fungizon®) for intravenous administration. Later, other formulations were introduced, including: a liposomal formulation (Ambisome ®), whereby AmB is present in a high state of aggregation, as well as in the lipid complex, Abelcet®; a colloidal dispersion, Amphocil®; and in an emulsion product in association with Intralipid®. These and other type of lipid-based formulations have been known to reduce the systemic toxicity without compromising the therapeutic efficacy of AmB [26-27]. It has been proposed that emulsion-based formulations that preserve and favor the release of the monomeric form of AmB below the critical concentration for self-association are less toxic than micellar suspensions [28]. Recently, it has also been shown that a heating treatment of AmB (20 min at 70 ˚C) combined with the formulation of a microemulsion leads to a new state of aggregation of AmB that exhibits lower toxicity and increases the in vitro and in vivo efficacy [29]. AmB also shows very low oral bioavailability due to its structural features that violate Lipinsky's rule (e.g., low Log P, high Mw, large polar surface area). Hence, novel pharmaceutical formulations of AmB are of great interest with a view to contribute to increase its pharmacological bioavailability for oral and other routes of administration, while exerting control on its drug release.

Scheme 1

EXPERIMENTAL SECTION

Materials

Cashew (Anacardium occidentale) gum exudate (CG) was kindly donated by EMBRAPA (Empresa Brasileira de Pesquisa Agropecuária, City, Brazil). It was isolated and purified according with the protocol previously developed by our Group [30]. CG was grafted with poly-L-lactide in two different CG:PLA molar ratio (1:1 and 1:10) as detailed by Reicher [19]. All chemical reagents were from Sigma-Aldrich (São Paulo, Brazil) and used without further purification. Amphotericin B was supplied by Ethycal (Fortaleza, Brazil). Dimethyl sulfoxide (DMSO) and acetone were from Synth (São Paulo, Brazil) and Miglyol 812® (coconut triglycerides of caprylic and capric fatty acids) was from Cremer Oleo (Witten, Germany).

Synthesis of Pickering Emulsions

The Pickering emulsions were prepared using the general principle of spontaneous emulsification, which is the fundamental principle for the preparation protocol of chitosan-based nanocapsules that have been extensively used in previous studies [31-32], though with modifications. Briefly, CGPLAP of the two different CG/PLA molar ratios (1:1 and 1:10) were initially fully dissolved in DMSO at 10 mg/mL. An aliquot of this solution poured into distilled water to a final volume of 20 mL and final three concentrations (0.5, 1.0 and 2.0 mg/mL). This led to the formation of nanoprecipitated particles of CGPLAP, thus comprising the aqueous phase. The organic phase consisted of 0.5 mL of ethanol, 125 µL of Miglyol and 9.5 mL of acetone. The organic phase (~10 mL) was immediately poured into the aqueous phase containing the CGPLAP self-assembled nanoparticles under quiescent conditions and the solution immediately turned milky. The solvents were subsequently evaporated in a rotavapor at 45°C. The thus obtained Pickering emulsion was isolated by centrifugation for 1 h at 25°C and at 15000 x G. The resulting milky cream on the solution was removed with a micropipette and stored under refrigeration until subsequent use. The emulsion type was determined by the

drop test [33]. Briefly, a drop of emulsion was added to either water or Miglyol and the ability of the sample to disperse was observed.

Characterization of physical properties

The particle size distributions of the CGPLAP nanoparticles and Pickering emulsions obtained from them were characterized by dynamic light scattering with non-invasive back scattering (DLS-NIBS) at 25°C upon irradiation of the sample with a 4 mW helium/neon red laser (λ=633 nm) and detection was at an angle of 173°. The zeta potential of the Pickering emulsions was measured by mixed laser Doppler velocimetry and phase analysis light scattering (M3–PALS). A Nanosizer ZS 3600 (Malvern Instruments Ltd., Worcestershire, UK) was used for both determinations. The samples were diluted 1:50 in water for size measurements and for zeta potential measurements.

Storage Stability

The storage stability of Pickering emulsions was determined in isolated formulations by measuring the particle size and polydispersity index using DLS-NIBS as described above. To this end, the emulsions were kept in refrigeration (~4 °C) and measurements were registered weekly [34].

Drug encapsulation

To encapsulate amphotericin B (AmB) into the Pickering emulsions, the same preparation procedure as described above was adopted, but with the variant that the drug was previously dissolved in DMSO together with the CGPLAP (1:1 and 1:10 CG:PLA molar ratio derivatives were used at copolymer concentration of 0.5 mg/mL) and added to the aqueous phase. The amount of AmB associated into the Pickering emulsion was determined by the subsequent extraction of the drug with DMSO from the isolated formulations. The emulsion was dissolved in a fixed aliquot of DMSO and vortexed for emulsion destruction and complete extraction of the drug. Amphotericin B concentration was measured using a spectrophotometer UV-visible (Shimadzu UV 1800) at λ=418 nm against a suitable calibration curve in DMSO.

ABS = 0.04450 -0.00671 c (1)

Where c is concentration in mg/mL. The AmB association efficiency was calculated from the following equation:

$$Association\ efficiency\ (\%) = \frac{[Total_{Drug}] - [Free_{Drug}]}{[Total_{Drug}]} \times 100$$

To determine the state of aggregation of AmB in Pickering emulsion before AmB extraction, Pickering emulsions with and without (as a blank) drug were diluted in deionized water and the UV/VIS spectrum was ran. The experiment was also performed with a commercial Sigma AMB solution (with sodium deoxycholate).

RESULTS AND DISCUSSION

Physical characteristics of nanoprecipitated CGPLAP nanoparticles

We hypothesized that the CG:PLA derivatives of low and high molar ratio would contribute to the formation and stabilization of Pickering o/w emulsions. To this end, we harnessed the self-assembly capacity of CGPLAP to form nanoparticles in an aqueous phase, along with that of spontaneous emulsification of an o/w emulsion by solvent displacement in the absence of added emulsifier. The expected structure of these Pickering emulsion systems is shown schematically in Figure 1.

Central to gleaning understanding of the formation process of the Pickering emulsion systems was first to examine the particle size distribution of the CGPLAP pre-formed particles obtained by nanoprecipitation and self-assembly upon blending polymer DMSO solutions with water (the non-solvent). The size distribution profiles, both in intensity or volume (%), of the nanoparticles obtained from the two derivatives of CGPLAP (1:1 and 1:10) at the three tested concentrations are shown in Figure 2.

Inspection of the size distribution profiles reveals that the particles formed by the CGPLAP derivative of lowest CG:PLA molar ratio (1:1) are strongly dependent on polymer concentration. The intensity (%) size distribution (Figure 2a) at c. 0.5 mg/mL shows a bimodal distribution with a predominant broad peak (centered at d. ~200 nm) and a smaller one (centered at d. ~6 nm). At 1.0 mg/mL though, these particle populations shift to d. ~550 and 50 nm, respectively. As the concentration increases to 2.0 mg/mL, only one population persists with an average diameter of ~550 nm. Similar trends are also reflected in the volume (%) distribution curves (Figure 2b), though as expected, the contribution of the smaller particles of the low and intermediate concentration is much more pronounced than in the intensity (%) profiles. In turn, the particles obtained by the CGPLAP of greater CG:PLA molar ratio (1:10), showed rather different concentration dependence in their intensity distribution profiles (Figure 2c). In this case, at the low and intermediate concentrations (0.5 and 1.0 mg/mL), three distinct populations were formed, each with average diameter values centered at ~8, ~80, and either ~800 (0.5 mg/mL) or ~500 nm (1.0 mg/mL). At the highest concentration, only one predominant peak centered at d. ~300 nm was observed, though a minor population of smaller size (d. ~10-20 nm) was also appreciated. The corresponding volume (%) size distribution profiles for these particles (Figure 2d) showed only one single peak with average d. ~7-8 nm, with negligible dependence on polymer concentration. To account for the differences in the size distribution profiles of the two derivatives as a function of concentration, it is necessary to discuss the nanoprecipitation process, particularly in terms of the phase separation phenomena that can be at play. Previous studies have addressed the role of the phase equilibrium and polymer solution thermodynamics on the nanoprecipitation complex process [36]. The experimental evidence from such previous studies is consistent with the notion that there is a direct relationship between the behavior of Flory´s interaction parameter and the dimensions of the nanoparticles. In our own study, the precise value of the Flory-Huggins parameter (χ) is unknown. Comparing the behavior of the two hydrophobic polysaccharide derivatives, CGPLAP 1:1 and 1:10, it appears that the concentration dependence is somewhat more pronounced for the less hydrophobic derivative. It can be expected that the polymer-solvent interactions be influenced by the degree of substitution and of polymerization of each derivative. Each of them would describe its own phase equilibrium diagram, and hence their dependence on concentration is expected to be different [37]. The more substituted hydrophobic derivative is likely to establish stronger interactions with DMSO, the organic solvent, than the less substituted

one. At the same time, if only the volume (%) size distribution profiles are considered, it is clear that the smaller particles are obtained at the lowest polymer concentration, namely 0.5 mg/mL for both derivatives. We examined the implications of the physical characteristics of the pre-formed particles on the formation and characteristics of the Pickering emulsions that comprised them, as discussed next.

Characteristics of the Pickering emulsions before and after isolation

The protocol to prepare Pickering emulsion systems consisted of two major steps, namely first preparing an aqueous phase comprised by CGPLAP nanoprecipitated particles, and by subsequent spontaneous emulsification upon blending the organic into the aqueous phase. The organic phase comprised Miglyol 812 (a biocompatible inert oil derived from coconut and palm), ethanol and acetone [31, 38]. Upon mixing the organic with the aqueous phase containing pre-formed nanoparticles of CGPLAP of the two CG:PLA molar ratio (1:1 and 1:10) at the varying concentrations, Pickering emulsion were spontaneously formed and stabilized by the adsorbed polysaccharide particles (Figure 1). The type of emulsion formed was oil-in-water type as confirmed by the droplet test after observing that the formulation dispersed immediately in water [33].

The particle size distribution profiles of the furnished Pickering emulsions before and after their isolation are shown in Figure 3 for the two distinct derivatives of low (1:1) and high (1:10) CG:PLA molar ratio. Inspection of the profiles for the freshly prepared emulsions (Figure 3a and 3b), reveals that the systems obtained from the nanoparticles made with CGPLAP (1:1) showed monomodal size distributions, when represented either in intensity or volume (%). Their Z-average diameter was ~450 nm and the distribution width spanned an order of magnitude (~100 to ~1000 nm). By contrast, the distribution curves for the freshly prepared systems obtained from CGPLAP (1:10), invariably exhibited two populations of particles, whose Z-average sizes were centered at d.~200 and ~3500 nm, regardless of whether the results were expressed in intensity or volume (%). In general, slight differences were noticed between size distribution profiles of freshly prepared and isolated systems both in intensity or volume (%) (Figure 3c and 3d, respectively). A moderate reduction in the overall size of the two systems is noticeable the consequence of isolation (see Figure 4 below). The monomodal and bimodal size distribution patterns observed, respectively, for the Pickering systems comprising

CGPLAP (1:1) and CGPLAP (1:10) nanoparticles, persisted even after the isolation process though.

The results of ζ-potential, Z-average size, and polydispersity, for all the freshly prepared and isolated Pickering emulsions of monomodal size distributions of CGPLAP at different CGPLAP concentrations are summarized in Figure 4. Notice that the ζ-potential values of freshly prepared systems (Figure 4a) decrease in a consistent trend from ζ ~-44 to ~-17 mV as the concentration of both CGPLAP (1:1) nanoparticles increases from 0.5 to 2.0 mg/mL. A closer inspection of the data showed that, on the one hand, at the CGPLAP (1:1) concentrations of 0.5 and 1.0 mg/mL, the isolation process results in a low change in ζ-. At the highest concentration (2 mg/mL) of CGPLAP (1:1), isolation brought about an increase in ζ-potential (from ~17 to ~-39 mV). In this latter case, the comparison between freshly prepared and isolated systems reveals that the magnitude of the relative increase in ζ-potential of the emulsions is proportional to the increase in concentration of the particles. Notice also that only negligible differences in ζ-potential are appreciable between isolated emulsions at the varying concentration of pre-formed nanoparticles of both CGPLAP derivatives.

As regard the Z-average diameter, inspection of the data in Figure 4c, reveals that as the concentration of CGPLAP nanoparticles increases, the dimensions of the freshly prepared Pickering emulsions grow by approximately two-fold (from ~300to ~900 nm). After isolation though, notice that the corresponding Z-average diameters for the emulsions furnished from nanoparticles of CGPLAP of concentration 0.5 mg/mL, showed only a slight reduction with regard to the freshly prepared systems . These differences grew gradually larger in both type of systems as the concentration increased to 1.0 and 2.0 mg/mL. Notice also on top of the Z-average size panels in Figure 4c, that the PDI values after isolation is about half of freshly prepared Pickering emulsion and also for both system it increase with concentration.

The physical characteristics of the Pickering emulsions formed by nanoparticles of the hydrophobic derivatives of cashew gum derivatives (Figure 3 and 4) described above seem to agree well with the notion that the pre-formed CGPLAP nanoparticles obtained by nanoprecipitation of the polysaccharide were amenable to stabilize oil-in-water Pickering emulsions upon adsorption of the small particles at the oil-water interface during the spontaneous emulsification process. Examination of the particle size distribution profiles of the Pickering emulsions (Figure 3) reveals that the more

homogeneous (i.e., monomodal size distributions) systems were furnished by nanoparticles of CGPLAP (1:1) rather than by those comprising CGPLAP (1:10) nanoparticles (bimodal distributions). Hence, we can argue that the optimal Pickering emulsions can be obtained using the 1:1 CGPLAP derivative at 0.5 mg/mL after isolation, having a Z-average diameter of 241±5 nm, PDI ~0.12±0.01, ζ-potential -40±5 mV.

The interpretation to these results stems on the particle size profiles of the pre-formed nanoparticles (Figure 2). The presence of predominantly too small a fraction of nanoparticles (d.~10 nm) in CGPLAP (1:1) seems to be key for the effective formation of Pickering emulsions. In turn, the systems obtained from already less homogeneous (bi-modal size distribution) pre-formed particles of CGPLAP (1:10), that seem to contain a fraction of large particles (d.~1000 nm), as expected, resulted in a non-monomodal particle size distributions. A plausible explanation to this bimodal distribution might be that at the two peaks correspond to a mixture between the Pickering emulsions and the unbound fraction of large CGPLAP (1:10) nanoparticles co-exist. However, the fact that after centrifugation the two populations still persisted, does not fully agree with this proposal. It is worth pointing out that the isolation of the emulsions upon centrifugation relies on the creaming separation of the droplets that remain at the surface, insofar as any matrix particles devoid of oil are bound to sediment at the bottom of the tube. Therefore, it seems unlikely that the population of large particle size corresponds to unbound CGPLAP (1:10) nanoparticles. If at all present, any surplus amount of large unbound particles would have settled down to the bottom of the tube upon centrifugation, and not remained in the close vicinity to the creamy layer of the emulsion. Therefore, we rather suggest the possibility of the existence two populations of Pickering emulsions of varying dimensions, namely one comprised by small and the other by large species; this suggestion seems more consistent with the experimental evidence. In the case of emulsions made from CGPLAP 1:1 nanoparticles, the size ratio of a polysaccharide particle-to-droplet is 0.011 (i.e., ~6 to ~550 nm), which is at the higher end of the typical size ratio of Pickering stabilized emulsions (i.e., 0.001 to 0.01) [39]. In the case of emulsions furnished by nanoparticles of CGPLAP 1:1 with larger Z-average size obtained at concentrations of 1.0 and 2.0 mg/mL, Pickering droplets of larger size were also formed (Figure 4).

The more detailed comparison of the characteristics of the Pickering emulsions furnished from CGPLAP nanoparticles at the different concentrations allowed to gain further insight into the mechanisms at play. As illustrated in Figure 4a, the behavior of the ζ-

potential of the different Pickering emulsions of freshly prepared systems decreased consistently with increasing concentration of the CGPLAP particles. It was extremely revealing to realize that the ζ-potential values attained by the freshly prepared emulsions of greater CGPLAP concentration matched closely those of the self-assembled nanoparticles (~-20 mV). This result is fully consistent with the idea that as the surface of the emulsions tends to be fully covered by CGPLAP nanoparticles, the ζ-potential of the emulsions should match that of the nanoparticles. Without further data for formulations at yet greater concentrations beyond 2 mg/mL, it is difficult to judge at this stage whether the surface of the emulsions became fully saturated with CGPLAP nanoparticles at such concentration.

Upon isolation, however, the physical characteristics of the Pickering emulsions changed dramatically as described above (Figure 4a). A plausible general explanation to account for the observed increase in ζ-potential after isolation, is that centrifugation causes desorption of the CGPLAP nanoparticles from the interface of the emulsions. Consistent with this view is the fact that at the greatest concentration (2 mg/mL), the magnitude of the difference (increase) is greatest. The apparent slight increase in ζ-potential of the Pickering droplets upon isolationcan be explained as the expected consequence of a less effective coverage of the emulsion surface. Miglyol 812® oil is known to be a mixture of triglycerides of caprilic and caproic acids derived from coconut and palm kernel. Even when the fatty acids in Miglyol occur predominantly as esterified as triglycerides, there is a small fraction of nonesterified fatty acids that confer the oil a slight acidity. The carboxylate groups of this small fraction of free fatty acids are bound to be fully exposed to the water phase, hence the highly negative ζ-potential of oil droplets. Therefore, the decrease in ζ-potential of the Pickering emulsions with increasing CGPLAP concentration, is consistent with the increase in the effective uncoated area of the oil droplets.

The available biophysical evidence presented above is consistent with the adsorption of the preformed CGPLAP nanoparticles to the interface of the o/w emulsion formed by solvent displacement. However, whether CGLAP nanoparticles disassemble upon adsorbing at the o/w interface and contribute to stabilize the emulsion due to the amphiphilic character of CGLAP, cannot be ruled out. Contact angle or FRET fluorescence measurements to probe the integrity of the nanoparticles during the

366 emulsification process would have shed further light into this issue, and are yet to be
367 considered in future studies.
368 Detachment of nanoparticles of CGPLAP from the interface upon centrifugation is also
369 fully consistent with the observed overall decrease in Z-average size (Figure 4c). We
370 reasoned that if the Pickering emulsions were conceived to be structured as schematically
371 shown in Figure 1, it would be expected that their dimensions be influenced by the corona
372 of putatively adsorbed nanoparticles. Hence, detachment of these nanoparticles from the
373 interface driven by the centrifuge force would be expected to result in a noticeable
374 decrease in size. A rough analysis of the size data shows that at the highest concentration
375 of 2.0 mg/mL, the Z-average size decreases from ~900 to ~500 nm. The magnitude of
376 this difference (~400 nm) is many-fold larger than the Z-average diameter of the
377 nanoparticles thought to be adsorbed at the interface (~6 nm). Given this large difference,
378 it might be that not a single but several layers of nanoparticles are adsorbed so as to
379 account for such too thick an interface.
380 The free energy required for desorption of particles is known to be given by the following
381 equation [40]:
382
383 $$E = \quad r^2\left(1 \quad |\cos \quad |\right)^2 \qquad (2)$$
384
385 where, γ is the oil-water surface tension, r is the radius of the particle, and θ is the contact
386 angle between the liquid and a solid substrate comprising of the same material as that for
387 the particle. In general, this energy is much greater than the sole thermal energy (k_BT),
388 even for small particles. Hence, particles once adsorbed at the interface, are very difficult
389 to displace. This is the reason behind the high efficacy of nanoparticles as stabilizers of
390 colloids such as emulsions and foams.
391 Even when the adsorption of particles at Pickering interfaces is often irreversible, the
392 application of external fields, has been shown to allow detachment of magnetic or
393 electrically polarizable particles [41]; [42]. Also, it has been argued that a higher density
394 of particles relative to the surrounding medium may be enough to detach particles from
395 bubbles [43]. In our work, we suggest that the centrifuge force causes the emulsion
396 droplets to rise while the particles are pulled down by the gravitational force, under a
397 similar process as the cited example for Pickering stabilized bubbles. The fact that the
398 differences in Z-average size and ζ-potential are magnified as the concentration of

CGPLAP nanoparticles increases, is consistent with the latter view in that a higher density of particles relative to the surrounding medium, favors their detachment from the interface.

Stability of Pickering emulsions in storage conditions

The stability of the isolated Pickering emulsions CGPALP 1:1 during their storage at 4˚C was assessed from the evolution of the Z-average size (Figure 5). Notice in Figure 5 that for the emulsions formed with CGPLAP 1:1 nanoparticles at the three explored concentrations, the Z-average size of the emulsions remained constant for up to 28 days. The trend in Z-average size at the three concentrations is similar to that observed in water for freshly prepared and isolated particles (Figure 4). Overall, the formulations appear to be stable during storage at refrigeration temperature. This is a result of practical significance, as it anticipates that the formulations could be stored for almost one month under refrigeration.

Amphotericine B (AmB) encapsulation and loading efficicency

The other important aspect to evaluate for the CGPLAP nanoparticles-stabilized Pickering emulsions was their capacity to associate AmB, which is a drug of low water solubility. Therefore, to load AmB into the formulations (aAlthough the bimodal size distribution observed for CGPLAP 1:10 it was also tested to encapsulate AmB), we chose the condition of CGPLAP nanoparticles at 0.5 mg/mL and the drug was loaded in the aqueous phase dissolved in DMSO. As shown above, this concentration of CGPLAP afforded optimal physical characteristics for the formation of Pickering emulsions.
The appreciable change in color from a milky white to a yellowish emulsion upon pouring the organic into the aqueous phase, along with the absence of formation of a precipitate, gave a first hint that AmB incorporated into the formulations successfully.

In aqueous media and at low concentrations (5.0×10^{-7} M aqueous solution), the UV/VIS spectrum of AmB showed four absorbance bands in the λ range from 320 to 450 nm. Three distinct major absorption bands are centered at λ ~375, ~395, and ~418 nm, and a flat small shoulder at λ~357 nm[28]; [44].

In general, the spectral changes induced by the aggregation of AmB may be represented as the value of the ratio of the intensities of the major absorption bands at λ=380 and 409 nm (i.e., ~ A_{350}/~A_{409} ratioThis ratio assumes a value of ~ 2.0 for AmB aggregated species, and of ~0.25 for the monomeric form [45-46]. In commercial formulations of AmB (e.g., Ambizone® and Fungizone®) A_{350}/A_{409} ratios of 2.9 and 4.8 have been determined, respectively [47], thus reflecting that AmB occurs in the aggregated form in such both cases.

Table 1 summarizes the data corresponding to the association of AmB into the Pickering emulsions obtained from the two different nanoparticles of CGPLAP 1:1 and 1:10. Comparison of the drug association efficiency for both type of formulations, reveals that the entrapment of AmB increases with the loading, particularly for the systems comprising nanoparticles of CGPLAP 1:10 that increase the association efficiency of AmB by nine-fold upon doubling the amount of loaded drug. By contrast, the magnitude of the increment of associated AmB due to the increase in AmB initial mass for the systems comprising nanoparticles of CGPLAP 1:1 was moderate (only ~20%), though the AmB association efficiency of the formulations with 5 mg of AmB was more than three-fold greater than that of the systems comprising nanoparticles of CGPLAP 1:10 at equivalent loading.

To make sense of the drug association results of AmB-loaded Pickering emulsions, it is worth to discuss in closer detail the protocol used to formulate these systems. Due to the restrictions imposed by the low solubility of AmB neither in ethanol or acetone, it was not possible to load it into the oil core of the nanoemulsions, as it would have been the ideal case. Hence, AmB had to be dissolved in the DMSO solution needed to dissolve CGPLAP. Upon mixing such solution in water, this led to the formation of nanoprecipitated polysaccharide particles. These particles were subsequently used to stabilize the Pickering emulsion droplets upon mixing the aqueous into the organic phase as already discussed above. Upon precipitation of CGPLAP particles driven by the phase equilibrium of the CGPLAP solvent (DMSO) and non-solvent (water), it would be

expected that AmB associates preferentially with the hydrophobic core of the CGPLAP nanoparticles, while contributing to reinforce hydrophobic associations. This would be consistent with the abrupt increase in association efficiency for the systems comprising CGPLAP 1:10 nanoparticles observed upon increase in drug loading, when compared to those comprising nanoparticles of CGPLAP 1:1. We venture to suggest that under this scenario, AmB would remain associated to the nanoparticles sitting at the oil-water interface of the stabilized Pickering emulsions. Yet an alternative possibility would be that upon creation of the emulsions, unassociated AmB remaining in the aqueous phase, may prefer to migrate to the oily core of the emulsions, under a similar mechanism that drives the spontaneous formation of the emulsion droplets (i.e., solvent displacement). Upon mixing the organic into the aqueous phase, acetone and ethanol instantaneously move to the aqueous phase, leaving depleted the oil droplets phase. However, free AmB in the aqueous phase might also get trapped into the newly formed oil droplets.

Yet another important aspect of notice was that upon centrifugation the Pickering emulsions to isolate them, a yellow colored pellet was observed at the bottom of the vials (See Figure S1 Supporting Information). This could be diagnostic of the presence of either precipitated AmB or unbound CGPLAP nanoparticles. Therefore, it stands to reason that AmB partitions itself between the emulsion droplets (either in the CGPLAP nanoparticles or at the core), a free fraction in the subnatant and the insoluble pellet that settles down upon centrifugation. At present, we have no experimental evidence to elucidate further the mechanisms at play nor to probe the preferred localization and molecular organization of AmB in the Pickering emulsions (i.e., whether it occurs in the oil core or at the adsorbed CGPLAP nanoparticles), but this can be the focus of future studies (e.g., using a fluorescent tagged AmB, as in previous studies) [48].

The UV-vis spectrum for 1: 1 and 1:10 GCPLAP AmB loaded emulsions and for a solution of commercial Sigma AmB in waterare shown in Figure 6. The spectrum shows a broad band at maximum intensity in 336 nm and 340 nm for derivatives 1: 1 and 1:10, respectively. Spectra with similar absorption profiles are found in chitosan and dextran sulfated nanoparticles [49] and in lipid complexes composed of DMPC and DMAC [50]. For CGPLAP emulsions 1: 1 and 1:10 a small displacement between bands (I) and (IV) was observed (340 and 342 nm lengths for the band (I) and 407 and 406 nm for the band (IV), for the 1: 1 and 1:10 derivatives, respectively). The I/IV ratio for CGPLAP 1: 1 and CGPLAP 1:10 was 1.7 and 1.6 respectively while for a commercial AmB solution the ratio was 2.5, indicating that the AmB is not fully aggregated within the emulsion

formulation. For the sulfated chitosan and dextran nanoparticles, the I/IV ratio found was 3.6 [49]. Commercial formulations such as Amphocil®, Fungizone®, Abelcet® and Ambisone® were found in the aggregate form (at 5% dextrose) with I/IV ratios of 9.1, 4.8, 1.3 and 2.9, respectively [47,51]. So, when compared with commercial formulations it seems that the Pickering formulations protect AmB against more extensive aggregation. This is a remarkable result particularly due to the importance of the aggragate form on the increase of toxicity.

CONCLUSION

In summary, in this work, we give proof-of-concept of the feasibility to prepare a Pickering emulsion system based on a hydrophobic derivative of cashew gum polysaccharide. To this end, nanoprecipitated polysaccharide particles were subsequently adsorbed at the interface of oil in water emulsions obtained by solvent displacement. As expected, the characteristics of the nanoparticles influence those of the Pickering emulsions. The route of preparing these systems offers the possibility to associate amphotericin B into these systems and associate it with efficiencies up to ~47% and presumably in less aggregated form than commercial formulations. Subsequent studies will examine the in vitro release and toxicity of these novel formulations.

Acknowledgement

The authors are grateful to CNPq (Brazil), CAPES (Brazil), INOMAT/INCT (Brazil), and FUNCAP (Brazil) for financial support in the form of grants and fellowships.

REFERENCES

[1] B.P. Binks, **Colloidal particles at liquid interfaces**, Phys. Chem. Chem. Phys. 9 (2007), pp 6298-6299.

[2] R. Aveyard, B.P. Binks and J.H. Clint, **Emulsions stabilised solely by colloidal particles**, Adv. Colloid Interface Sci. 100–102 (2003), pp. 503-543.

[3] CY. Zhou, H. Li, H. Zhou, H. Wangm PJ. Yang and SA Zhong, **Water-compatible halloysite-imprinted polymer by Pickering emulsion polymerization for the selective regognition of herbicides**, J. Sep. Sci. 38 (2015), pp 1365-1371.

[4] Y. Sun, J. Chen, Y. Li, H. Li, X. Zhu, Y. Hu, S. Huang, J. Li, S. Zhong, **Bio-inspired magnetic molecularly imprinted polymers based on Pickering emulsions for selective protein recognition**, New J. Chem. 40 (2016) 8745–8752

[5] Y. Sun, S. Zhong, **Nanoscale trifunctional bovine hemoglobin for fabricating molecularly imprinted polydopamine via Pickering emulsions-hydrogels polymerization**, Colloids Surf., B. 159 (2017) 131–138.

[6] Y. Sun, Y. Li, J. Xu, L. Huang, T. Qiu, S. Zhong, **Interconnectivity of macroporous molecularly imprinted polymers fabricated by hydroxyapatite-stabilized Pickering high internal phase emulsions-hydrogels for the selective recognition of protein**, Colloids Surf., B. 155 (2017) 142–149.

[7] Y. Wei, J. Chen, Z. Lu, **Color changing Pickering emulsions stabilized by polysiloxane microspheres bearing phenolphthalein groups**, RSC Adv. 5 (2015) 71824–71829.

[8] F. Nan, J. Wu, F. Qi, Y. Liu, T. Ngai and G. Ma, **Uniform chitosan-coated alginate particles as emulsifiers for preparation of stable Pickering emulsions with stimulus dependence**, Colloids Surf., A. 456 (2014) pp. 246-252.

[9] X. Song, Y. Pei, M. Qiao, F. Ma, H. Ren and Q. Zhao, **Preparation and characterizations of Pickering emulsions stabilized by hydrophobic starch particles**, Food Hydrocolloids. 45 (2015), pp. 256-263.

[10] A. Yusoff, and B.S. Murray, **Food Hydrocolloids Modified starch granules as particle-stabilizers of oil-in-water emulsions**, Food Hydrocolloids. 25 (2011), pp. 42-55.

[11] M. V Tzoumaki, T. Moschakis, V. Kiosseoglou and C.G. Biliaderis, **Food Hydrocolloids Oil-in-water emulsions stabilized by chitin nanocrystal particles**, Food Hydrocolloids. 25 (2011) 1521-1529.

[12] W.W. Mwangi, K.W. Ho, B.T. Tey and E.S. Chan, **Effects of environmental factors on the physical stability of pickering-emulsions stabilized by chitosan particle**s, Food Hydrocolloids. 60 (2016), pp. 543-550.

[13] J.O. Zoppe, R. a. Venditti and O.J. Rojas, **Pickering emulsions stabilized by cellulose nanocrystals grafted with thermo-responsive polymer brushes**, J. Colloid Interface Sci. 369 (2012), pp. 202-209.

[14] C. Wen, Q. Yuan, H. Liang and F. Vriesekoop, **Preparation and stabilization of D-limonene Pickering emulsions by cellulose nanocrystals**., Carbohydr. Polym. 112 (2014), pp. 695-700.

[15] M. Visanko, H. Liimatainen, J.P. Heiskanen and O. Hormi, **Amphiphilic Cellulose Nanocrystals from Acid-Free Oxidative Treatment: Physicochemical**

Characteristics and Use as an Oil − Water Stabilizer, Biomacromolecules. 15(2014), pp. 2769-2775.

[16] F. Liu, C. **Tang, Soy Protein Nanoparticle Aggregates as Pickering Stabilizers for Oil- in-Water Emulsions**, J. Agric. Food Chem. 61 (2013), pp 8888–8898.

[17] M. Destribats, M. Rouvet, C. Gehin-Delval, C. Schmitt and B.P. Binks, **Emulsions stabilised by whey protein microgel particles: towards food-grade Pickering emulsions**., Soft Matter. 10 (2014), pp. 6941-6954.

[18] R.C.M. de Paula, F. Heatley and P.M. Budd, Characterization of Anacardium occidentale Exudate Polysaccharide, Polym. Int. 45 (1998), pp. 27-35..

[19] A.R. Richter, Síntese e caracterização de emulsões de Pickering a base de goma do cajueiro enxertado com lactídeo, Universidade Federal do Ceará, Ceará, 2015.

[20] L. Dai, D. Li and J. He, **Degradation of graft polymer and blend based on cellulose and poly(L-lactide)**, J. Appl. Polym. Sci. 130 (2013) 2257.

[21] K. Nagahama, T. Ouchi and Y. Ohya, **Biodegradable nanogels prepared by self-assembly of poly(L-lactide)-grafted dextran: Entrapment and release of proteins**, Macromol. Biosci. 8 (2008), pp. 1044-1052.

[22] N. GOLD, H. A. Stout, J. F. Pagano and R. Donovick, **Amphotericin A and B, antifugal antibiotics produced by a streptomycete I. in vivo studies**. Antibiotics Annual. 1955 (1956), pp. 579-586.

[23] R.J. Hamill, **Amphotericin B formulations: A comparative review of efficacy and toxicity**, Drugs. 73 (2013), pp. 919-934.

[24] B. De Kruijff, W.J. Gerritsen, A. Oerlemans, R.A. Demel and L.L.M. van Deenen, **Polyene antibiotic-sterol interactions in membranes of Acholeplasma laidlawii cells and lecithin liposomes. I. Specificity of the membrane permeability changes induced by the polyene antibiotics**, Biochim. Biophys. Acta, Biomembr. 339 (1974), pp. 30-43.

[25] P. Legrand, E.A. Romero, B.E. Cohen and J. Bolard, **Effects of aggregation and solvent on the toxicity of amphotericin B to human erythrocytes**, Antimicrob. Agents Chemother. 36 (1992), pp. 2518-2522.

[26] L. C. Souza, R. C. Maranhão, S. Schreier and A. Campa, **In-vitro and in-vivo studies of the decrease of amphotericin B toxicity upon association with a triglyceride-rich emulsion.** J. Antimicrob. Chemother. 32 (1993), pp. 123-132.

[27] S. Jullien, A. Contrepois, J.E. Sligh, Y. Domart, P. Yeni, J. Brajtburg, G. Medoff and J. Bolard, **Study of the effects of liposomal amphotericin B on Candidaalbicans, Cryptococcusneoformans, and erythrocytes by using small unilamellar vesicles prepared from saturated phospholipids**, Antimicrob. Agents Chemother. 33 (1989), pp. 345-349.

[28] E.S.T. Do Egito, H. Fessi, M. Appel, G. Barratt, P. Legrand, J. Bolard and J.P. Devissaguet, **A morphological study of an amphotericin B emulsion-based delivery system**, Int. J. Pharm. 145 (1996), pp.17-27.

[29] M.A. da Silva-Filho, S.D.V. da S. Siqueira, L.B. Freire, I.B. de Araújo, K.G. de Holandae e Silva, A.C. da Medeiros, I. Araújo-Filho, A.G. de Oliveira and E.S.T. do Egito, **How can micelle systems be rebuilt by a heating process?**, Int. J. Nanomed. 7 (2012), pp. 141- 150.

[30] J.F. Rodrigues, R.C.M. De Paula and S.M.O. Costa, **Métodos de Isolamento de Gomas Naturais : Comparação Através da Goma do Cajueiro (Anacardium occidentale L)**, Polim.: Cienc. Tecnol. 16 (1993),pp. 31-36.

[31] F.M. Goycoolea, A. Valle-Gallego, R. Stefani, B. Menchicchi, L. David, C. Rochas, M.J. Santander-Ortega and M.J. Alonso, **Chitosan-based nanocapsules: Physical characterization, stability in biological media and capsaicin encapsulation**, Colloid Polym. Sci. 290 (2012), pp. 1423- 1434.

[32] M. Kaiser, S. Pereira, L. Pohl, S. Ketelhut, B. Kemper, C. Gorzelanny, H.-J. Galla, B.M. Moerschbacher and F.M. Goycoolea, **Chitosan encapsulation modulates the effect of capsaicin on the tight junctions of MDCK cells.,** Sci. Rep. 5 (2015) 10048.

[33] J.O. Zoppe, R.A. Venditti, O.J. Rojas, **Pickering emulsions stabilized by cellulose nanocrystals grafted with thermos-responsive polymer brushes**, J. Colloid Interface Sci. 369 (2012), pp. 202 – 209.

[34] F.M. Goycoolea, F. Brunel, N.E. El Gueddari, A. Coggiola, G. Lollo, B.M. Moerschbacher, C. Remuñán-López, T. Delair, A. Domard, M.J. Alonso, Physical **Properties and Stability of Soft Gelled Chitosan-Based Nanoparticles**, Macromol. Biosci. (2016), pp 1 - 10.

[35] M. Costalat, L. David and T. Delair, **Reversible controlled assembly of chitosan and dextran sulfate: A new method for nanoparticle elaboration**, Carbohydr. Polym. 102 (2014), pp. 717-726.

[36] S. Galindo-Rodriguez, E. Allémann, H. Fessi and E. Doelker, **Physicochemical parameters associated with nanoparticle formation in the salting-out, emulsification-diffusion, and nanoprecipitation methods**, Pharm. Res. 21 (2004), pp. 1428-1439.

[37] A. Luque-Alcaraz, J. Lizardi-Mendoza, F. Goycoolea, I. Higuera-Ciapara and W. Argüelles-Monal, **Preparation of chitosan nanoparticles by nanoprecipitation and their ability as a drug nanocarrier**, RSC Adv. 6 (2016), pp. 59250-59256.

[38] F. a. Oyarzun-Ampuero, G.R. Rivera-Rodriguez, M.J. Alonso and D. Torres, **Hyaluronan nanocapsules as a new vehicle for intracellular drug delivery**, Eur. J. Pharm. Sci. 49 (2013), pp. 483-490.

[39] R. Ettelaie and S. V Lishchuk, **Detachment force of particles from fluid droplets**, Soft Matter. 11 (2015), pp. 4251-4265.

[40] S. U. Pickering, **CXCVI.-Emulsions**.. J. Chem. Soc., Trans., (1907), 91, 2001–2021.

[41] K. Hwang, P. Singh and N. Aubry, **Destabilization of pickering emulsions using external electric fields**, Electrophoresis. 31 (2010), pp. 850-859.

[42] E. Kim, K. Stratford and M.E. Cates, **Bijels containing magnetic particles: A simulation study**, Langmuir. 26 (2010), pp. 7928-7936.

[43] J. W. Tavacoli, G. Katgert, E. G. Kim, M. E. Cates and P. S. Clegg, **Size Limit for Particle-Stabilized Emulsion Droplets under Gravity**, Phys. Rev. Lett., 108 (2012) 268306.

[44] J. Bolard, M. Seigneuret and G. Boudet, **Interaction between phospholipid bilayer membranes and the polyene antibiotic amphotericin B**, Biochim. Biophys. Acta, Biomembr. 599 (1980), pp. 280-293.

[45] J. Barwicz, S. Christian and I. Gruda, **Effects of the aggregation state of amphotericin B on its toxicity to mice**, Antimicrob. Agents Chemother. 36 (1992), pp. 2310-2315.

[46] G. Vandermeulen, L. Rouxhet, A. Arien, M.E. Brewster and V. Préat, **Encapsulation of amphotericin B in poly(ethylene glycol)-block-poly(ε-caprolactone-co-trimethylenecarbonate) polymeric micelles**, Int. J. Pharm. 309 (2006), pp. 234-240.

[47] K.K. Nishi, M. Antony, P. V. Mohanan, T. V. Anilkumar, P.M. Loiseau and A. Jayakrishnan, **Amphotericin B-gum arabic conjugates: Synthesis, toxicity, bioavailability, and activities against Leishmania and fungi**, Pharm. Res. 24 (2007), pp. 971- 980.

[48] J. P. Jain and N Kumar, **Development of amphotericin B loaded polymersomes based on (PEG)3-PLA co-polymers: Factors affecting size and in vitro evaluation**. Eur. J. Pharm. Sci. 40 (2010), pp. 456-465.

[49] W.Tiyaboonchai and N. **Formulation and characterization of amphotericin B-chitosan-dextran sulfate nanoparticles**. Int. J. Pharm. 329 (2007), pp. 142-149.

[50]

[51] A.B. Mullen, K.C. Carte and A.J. Baillie, **Comparison of the efficacies of various formulations of amphotericin B against murine visceral leishmaniasis**. Antimicrob. Agents Chemother. 41 (1997), pp. 2089-2092.

FIGURES AND TABLES

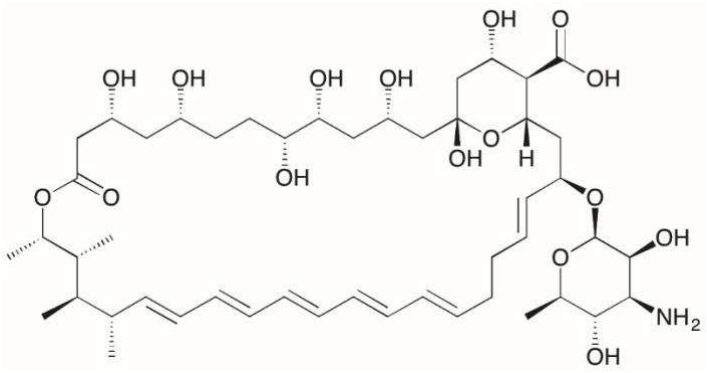

Scheme 1. Structure of AmB

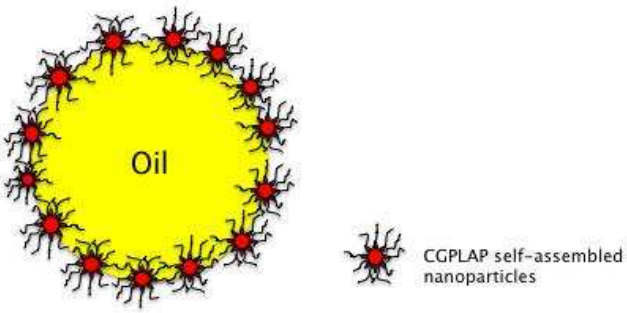

Figure 1. Schematic illustration of the Pickering emulsion stabilized by CGPLAP self-assembled nanoparticles. The red core of the CGPLAP nanoparticles, represents the hydrophobic regions, while the black lines, do the hydrophilic polysaccharide.

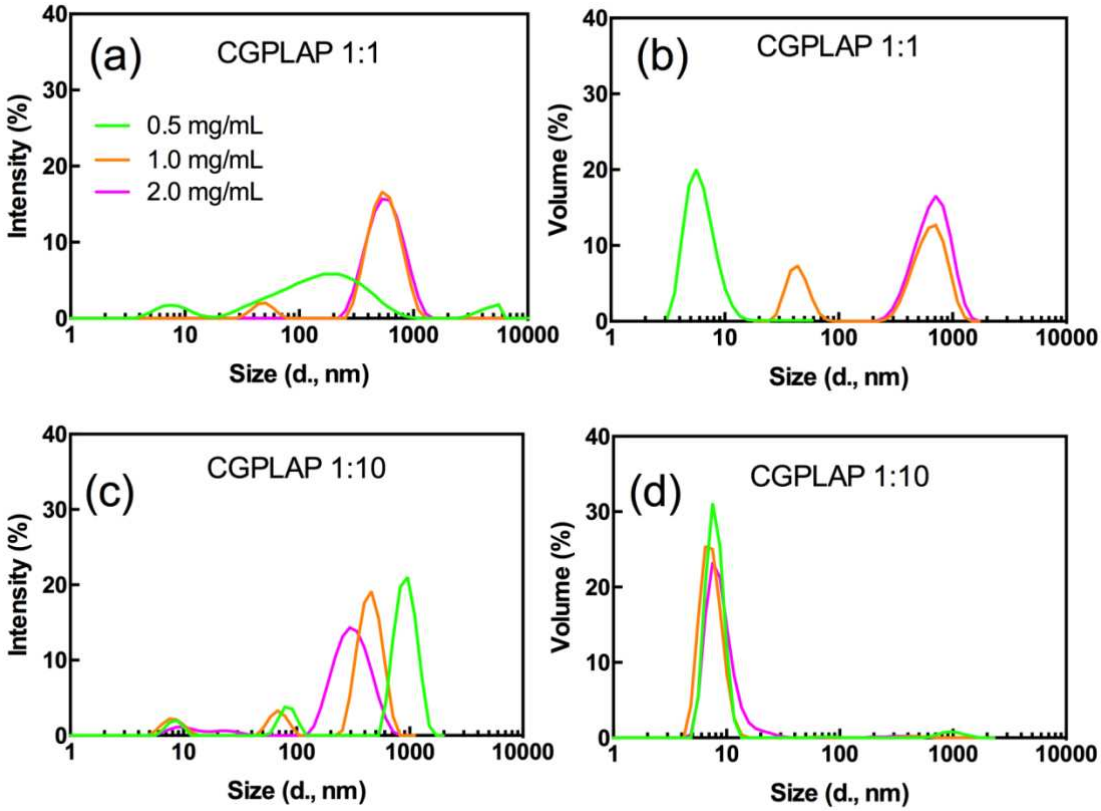

754

755

756 **Figure 2.** Size distribution profile of NP´s (a) CGPLAP 1:1 in intensity, (b) CGPLAP 1:1
757 in volume, (c) CGPLAP 1:10 in intensity and (d) CGPLAP 1:10 in volume (size and
758 standard deviation by intensity and volume (%) are depicted in Table A at supplementary
759 information).

760

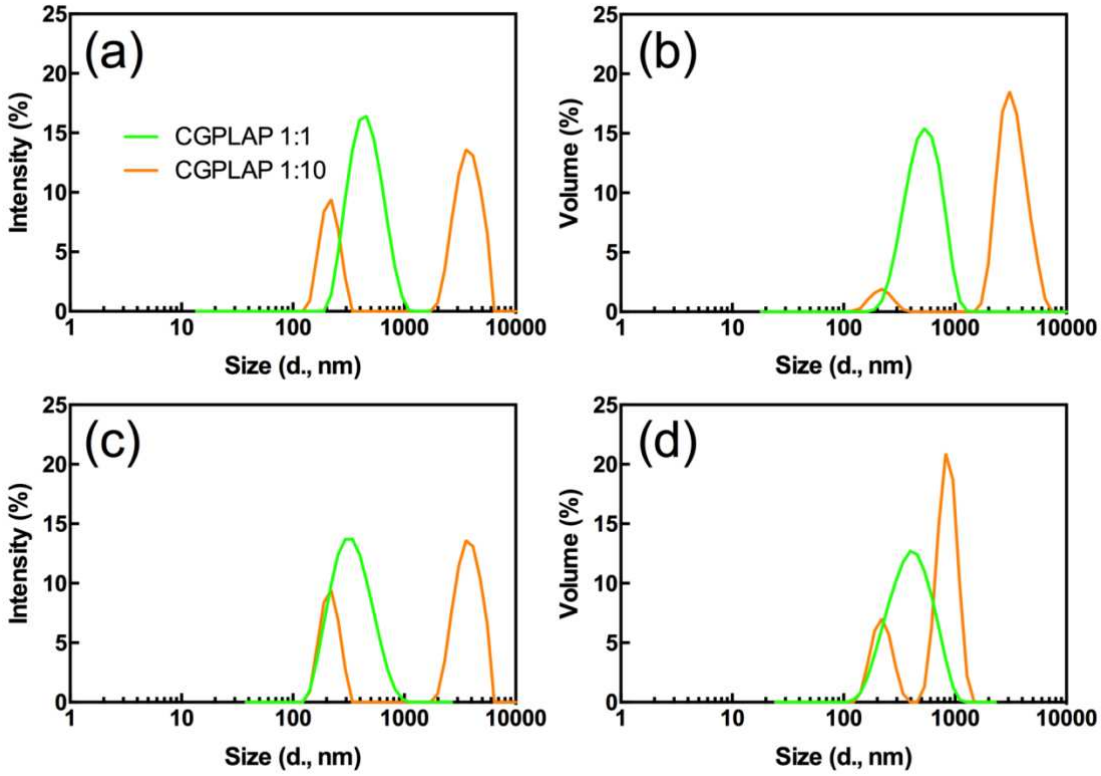

761

762 **Figure 3.** Size distribution profile of Pickering emulsions stabilized by CGPLAP
763 nanoparticles (0.5 mg/mL). Freshly prepared: (a) in intensity and (b) in volume; and
764 Isolated: (c) in intensity and (d) in volume(size and standard deviation by intensity and
765 volume (%) are depicted in Table B at supplementary information)

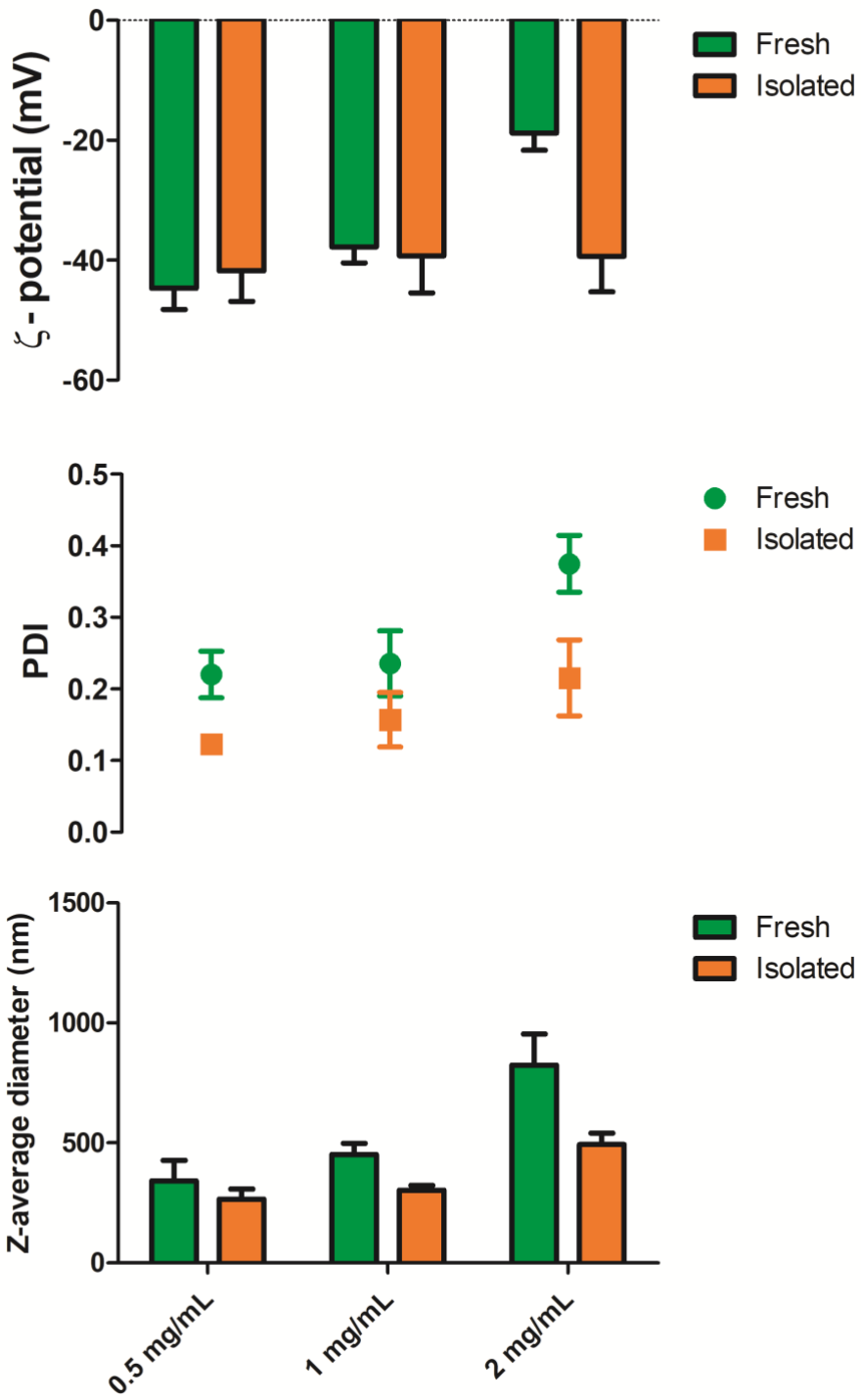

766

767

768

769 **Figure 4.** ζ- potential for (a) Fresh, (b) Isolated, Z-average size and Polydispersity for (c)
770 fresh and (d) isolated Pickering Emulsion (mean average values ± SD; different letters in
771 bars denote significant differences among treatments $p \leq 0.05$ after unpaired t-tests; n =
772 3).

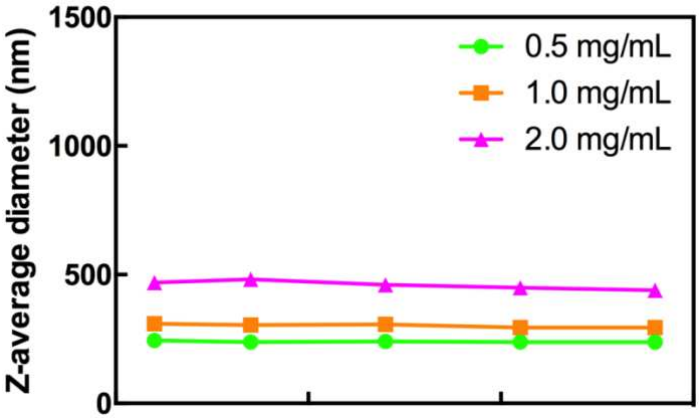

Figure 5 . Stability of the isolated Pickering emulsion during storage at 4 °C. Systems comprising CGPLAP 1:1 (please add X lable)

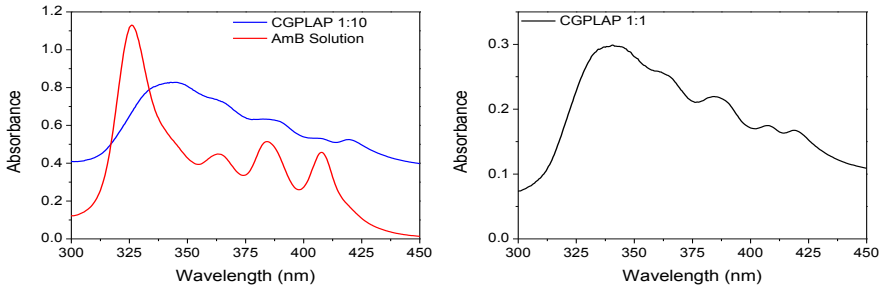

Figure 6. UV/VIS spectrum of AmB encapsulated in Pickering emulsion of CGPLAP 1:1 and CGPLAP 1:10 encapsulated and of commercial Sigma AmB solution

794

795

796

797 **Table 1.** Association of amphotericin B-loaded in Pickering emulsions
798 obtained from CGPLAP derivatives nanoparticles (0.5 mg/mL).

Formulation	Initial AmB (mg)	A.E.[1] (%)
CGPLAP 1:1	10	27.4±19
	5	21.1±7.9
CGPLAP 1:10	10	47.8±9.7
	5	5.7±5.6

799 [1]A.E.=Drug association efficiency

800

801

802